Journal of ELECTRONIC MATERIALS, Vol. 36, No. 12, 2007
DOI: 10.1007/s11664-007-0285-3

Regular Issue Paper

Creep Life Assessment of Tin-Based Lead-Free Solders Based on Imaginary Initial Strain Rate

KENJI MONDEN[1,2]

1.—Denki Kagaku Kogyo Kabushiki Kaisha (DENKA), 3-5-1 Asahimachi, Machida-shi, Tokyo 194-8560, Japan. 2.—e-mail: kenji-monden@denka.co.jp

The creep properties of tin-based, lead-free solders, Sn-3.0Ag-0.5Cu and Sn-7.5Zn-3.0Bi, were investigated for the temperature range from 298 K to 398 K. The creep rupture time decreases with increasing initial stress and temperature. The Omega method is applied to the analysis of the solder creep curves. The creep rate $\dot{\varepsilon}$ is expressed by the following formula: $\ln \dot{\varepsilon} = \ln \dot{\varepsilon}_0 + \Omega\varepsilon$, where $\dot{\varepsilon}_0$ and Ω are experimentally determined. The parameter $\dot{\varepsilon}_0$, the imaginary initial strain rate, increases with increasing initial stress and temperature. The parameter Ω is temperature dependent, but less dependent on the initial stress. The apparent activation energy for $\dot{\varepsilon}_0$ is 108 kJ/mol in Sn-3.0Ag-0.5Cu and 83 kJ/mol in Sn-7.5Zn-3.0Bi. These values are close to the activation energy for the lattice diffusion of tin. The creep rupture time is calculated using the parameters $\dot{\varepsilon}_0$ and Ω. The calculated creep rupture time is in good agreement with the measured creep rupture time.

Key words: Creep life assessment, imaginary initial strain rate, lead-free solder

INTRODUCTION

Lead-free solders are replacing traditional tin–lead solders as part of a major trend toward protecting the Earth's environment. Since creep is the main deformation mechanism in solder joints, understanding the constitutive model for creep and examining creep data for lead-free solders are important for reliability analysis of solder joints. A steady-state creep equation is generally used for lead-free solders,[1,2] which supposes that the secondary, or minimum, creep rate occupies the entire creep life. However, secondary creep constitutes only about 15–40% of the entire creep life for lead-free solders. Thus, the equation may not represent the entire creep life.

Certain parametric methods[3,4] have been used to predict the creep rupture time of lead-free solders. The physical significance of parameters appearing in the parametric methods is not very clear because they are usually determined based on creep rupture data under constant load. In contrast to the parametric methods, a modified theta projection concept[5] is determined by fitting a creep curve under constant stress to a specific equation. However, the creep curve expressed by the modified theta projection concept is not well described near the failure point, and it underestimates the rupture strain.

In this study, the omega method, which was developed to deduce the state equation for creep under constant load and to predict the creep rupture time, is applied to the analysis of creep curves of tin-based lead-free solders. The adaptability of the method to the creep deformation of the lead-free solders Sn-3.0Ag-0.5Cu and Sn-7.5Zn-3.0Bi was also investigated. The Sn-3.0Ag-0.5Cu solder is one of the earliest commercially available lead-free solders. The Sn-7.5Zn-3.0Bi solder is expected to be used as a substitute for the tin-lead eutectic solder because its melting temperature is much closer to that of tin-lead eutectic solder than to those of the other lead-free solders, such as tin-silver alloys.

(Received January 15, 2007; accepted August 16, 2007; published online September 22, 2007)

EXPERIMENTAL

Specimen Preparation

The creep specimen was machined from a cylindrical ingot, 130 mm long and 30 mm in diameter. Table I shows the chemical composition of the solders used in this study. The composition was analyzed by X-ray fluorescence analysis. The dimension of each creep specimen is 25 mm in gauge section and 7.5 mm in diameter. The shape and dimensions of a creep specimen are shown in Fig. 1. Each specimen was subjected to two hours of heat treatment at a temperature corresponding to approximately 0.82 of the melting point temperature of each solder. The heat-treatment temperatures for Sn-3.0Ag-0.5Cu and Sn-7.5Zn-3.0Bi were 400 K and 380 K, respectively.

Creep Testing

The creep experiments in this study used a custom-built tension-creep apparatus. A gravity-loaded mechanical arm applied force to the sample, and calibrated weights were loaded onto the mechanical arm. The test load was applied as quickly as possible, to approximate the ideal creep experiment in which the load is applied instantaneously. The specimens were heated in a temperature chamber. The heating system maintained the temperature variation at less than 1 K.

The specimens have two collars at both the ends of the gage part. An extensiometer was attached to the two collars to measure the elongation of the gage part during the test. A linear variable differential transducer (LVDT) was directly linked to the extensiometer. A data-acquisition unit collected the signals from the LVDT.

To investigate the effects of temperature and initial stress, the creep tests were conducted at three different temperatures of 298, 343, and 398 K. The elongation and temperature were continuously recorded. The stress applied in the creep test, σ_0, was calculated based on the initial cross sectional area before the test.

RESULTS AND DISCUSSION

Imaginary Initial Strain Rate and Creep Equation

Shi and Endo[6,7] introduced the imaginary initial strain rate $\dot{\varepsilon_0}$ and the strain rate acceleration factor Ω, which is transcribed as S, to express the creep rate under constant load for prestrained 2.25Cr-1Mo steel. Similarly, Prager[8] proposed the omega method for characterizing the behavior of carbon steel after service, in a creep range independent of that of Shi and Endo.

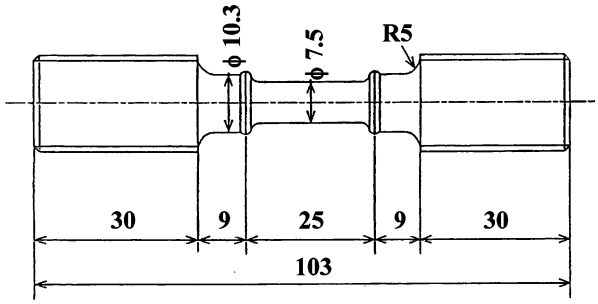

Fig. 1. Shape and dimensions of the creep test specimen in millimeters.

When the reloading creep stress is lower than that of the precreep, it suppresses the primary creep. Therefore, linearity between the logarithmic strain rate and true strain was obtained over almost the entire range of creep life. When the primary and secondary creep regimes are minimal and tertiary creep is dominant, the strain rate $\dot{\varepsilon_0}$ is expressed by the following formula:

$$\ln \dot{\varepsilon} = \ln \dot{\varepsilon_0} + \Omega\varepsilon, \tag{1}$$

where $\dot{\varepsilon_0}$ is the strain rate at $\varepsilon = 0$ and Ω is the slope of the line. Rewriting Eq. 1 and integrating it with respect to time from zero to t results in Eq. 2

$$\varepsilon = (1/\Omega)\ln[1/(1 - \Omega\dot{\varepsilon_0}t)]. \tag{2}$$

Using Eq. 2, the creep curve can be drawn if $\dot{\varepsilon_0}$ and Ω are known. We have that $t < 1/\Omega\dot{\varepsilon_0}$ from the constraint on the independent variable of the logarithmic function. Therefore, the rupture time t_r can be defined by the following equation:

$$t_r = (1/\Omega\dot{\varepsilon_0}). \tag{3}$$

Since tertiary creep is dominant in the tin-based lead-free solder, the omega method is applied to the analysis of the solder creep curves.

Creep Curve Properties

An example of the relationship between the logarithmic strain rate and true strain for Sn-3.0Ag-0.5Cu is shown in Fig. 2. As the tertiary creep is dominant in the tin-based lead-free solder Sn-3.0Ag-

Table I. Chemical Composition of Tested Lead-Free Solders in Mass Percent Ratio [%]

	Ag	Cu	Zn	Bi	Fe	Ni	Pb	Sn
Sn-3.0Ag-0.5Cu	2.7	0.45	N.D.	N.D.	0.01	0.01	0.02	Bal.
Sn-7.5Zn-3.0Bi	N.D.	N.D.	7.4	2.7	0.02	0.01	0.02	Bal.

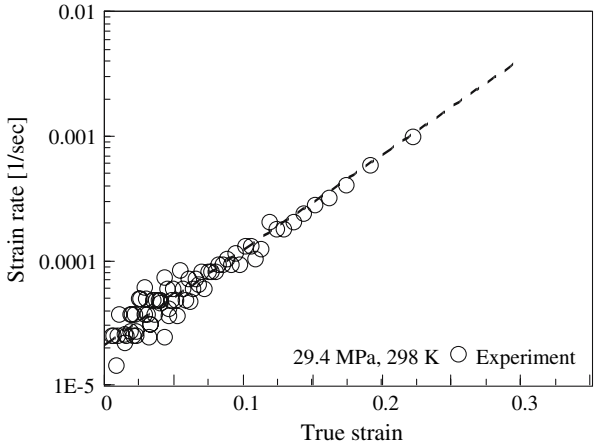

Fig. 2. Relationship between strain rate and true strain for Sn-3.0Ag-0.5Cu.

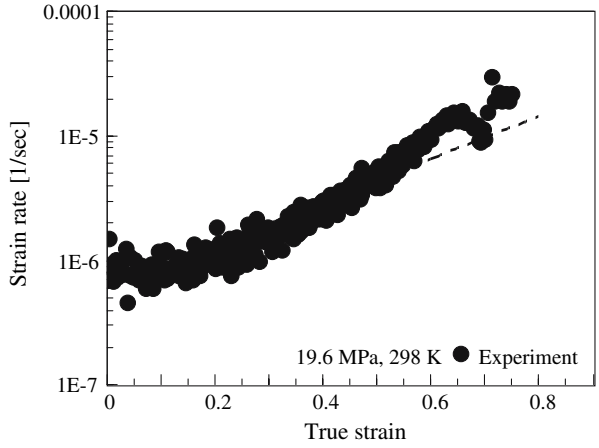

Fig. 4. Relationship between strain rate and true strain for Sn-7.5Zn-3.0Bi.

0.5Cu, linearity between the logarithmic strain rate and true strain was obtained over almost the entire range of creep life. The parameters $\dot{\varepsilon_0}$ and Ω are determined by least-squares regression to fit the data, as shown in Fig. 2. Figure 3 shows an example of a creep curve obtained in the present work for Sn-3.0Ag-0.5Cu. The line and the cross showing the rupture point are described by Eq. 2 using $\dot{\varepsilon_0}$ and Ω. The open circles are the experimental data. The calculated creep curve accurately describes the creep deformation and the rupture point.

An example of the relationship between the logarithmic strain rate and the true strain for Sn-7.5Zn-3.0Bi is shown in Fig. 4. Since the creep curve for Sn-7.5Zn-3.0Bi consists of slight primary creep and almost full tertiary creep, the omega method is applied to the analysis. Figure 5 shows an example of the creep curve obtained in the present study for Sn-7.5Zn-3.0Bi. The calculated creep curve accurately describes the creep deformation and the rupture point.

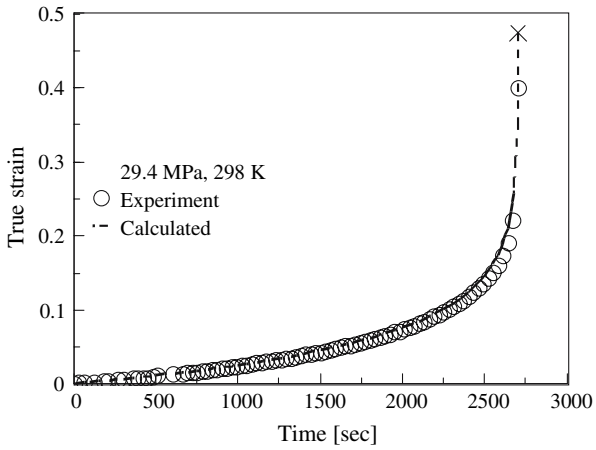

Fig. 3. Measured and calculated creep curves for Sn-3.0Ag-0.5Cu.

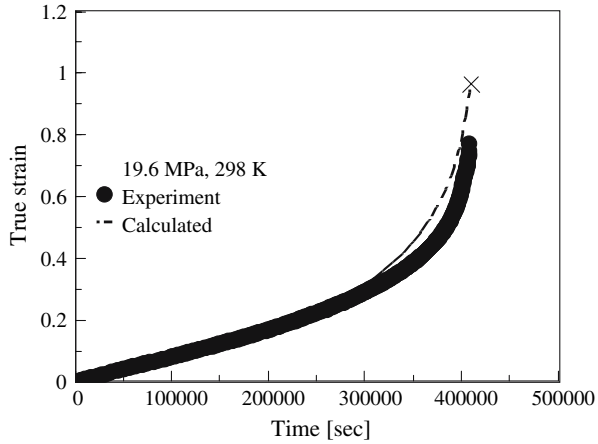

Fig. 5. Measured and calculated creep curves for Sn-7.5Zn-3.0Bi.

Effects of Stress and Temperature on the Parameters

When the primary and secondary creep regimes are minimal and tertiary creep is dominant, the relationship between the imaginary initial strain rate and the expected initial stress is shown as follows:[6]

$$\dot{\varepsilon_0} = A_0(\sigma_0/E)^{n_0}\exp(-Q_0/RT), \tag{4}$$

where A_0 = a constant factor, E = Young's modulus, n_0 = stress exponent, and Q_0 = apparent activation energy for imaginary initial strain rate, which is independent of stress provided that the normalized initial stress σ_0/E is used instead of σ_0. It is assumed that Eq. 4 gives a reasonable representation of the imaginary initial strain rate, which would be roughly equal to the secondary creep rate.

The effect of temperature on the imaginary initial strain rate for lead-free solders is shown in Fig. 6. The logarithmic imaginary initial strain rates $\ln \dot{\varepsilon_0}$ are plotted against the reciprocal temperatures $1/T$.

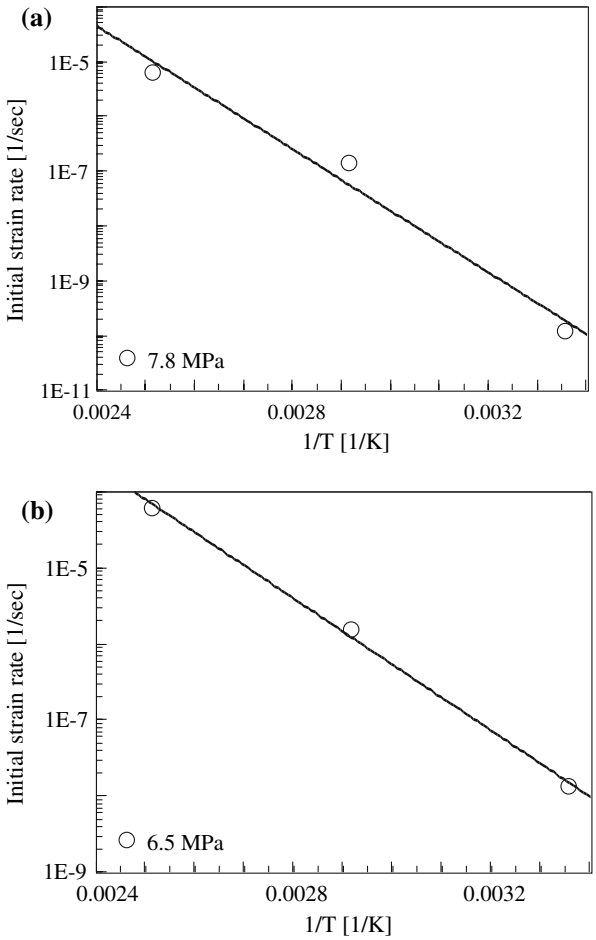

Fig. 6. Relationship between the imaginary initial strain rate and the reciprocal temperature for (a) Sn-3.0Ag-0.5Cu and (b) Sn-7.5Zn-3.0Bi.

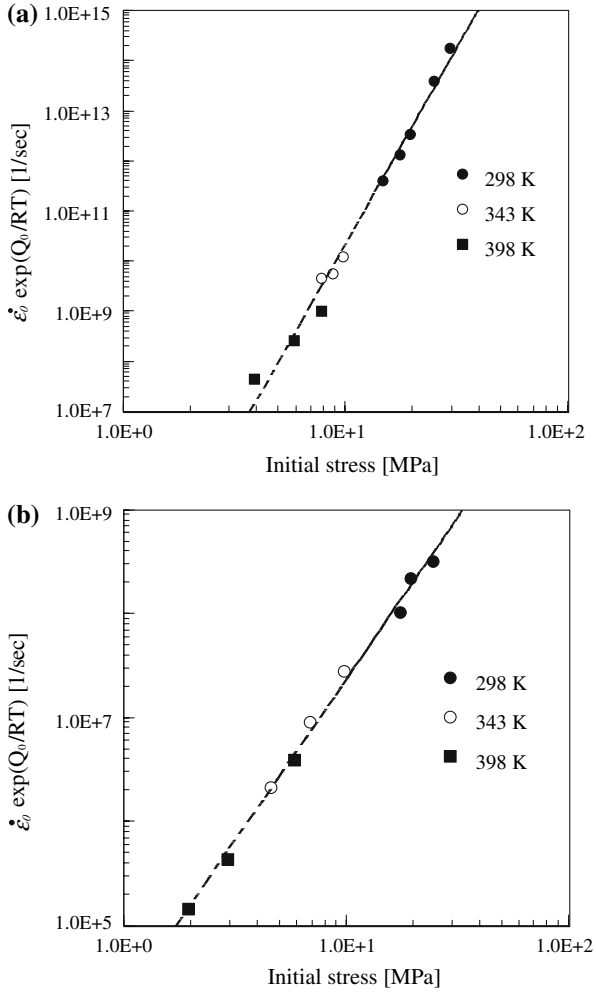

Fig. 7. Temperature-compensated imaginary initial strain rate as a function of the initial stress for (a) Sn-3.0Ag-0.5Cu and (b) Sn-7.5Zn-3.0Bi.

The relationship between $\ln \dot{\varepsilon}_0$ and $1/T$ appears to be linear, and the slope of the line gives the value $-Q_0/R$. The apparent activation energy for the imaginary initial strain rate of Sn-3.0Ag-0.5Cu is 108 kJ/mol under a constant stress of 7.8 MPa. That of Sn-7.5Zn-3.0Bi is 83 kJ/mol under a constant stress of 6.5 MPa. These values are close to the activation energy for the lattice diffusion of tin, 104 kJ/mol.[9]

The value $\dot{\varepsilon}_0 \exp(Q_0/RT)$ is plotted against the initial stress σ_0 in Fig. 7. All data points fall in the vicinity of a single line. This fact demonstrates explicitly that there exists a state equation for the imaginary initial strain rate. The slope of the line represents n_0. The parameter $\dot{\varepsilon}_0$ increases as the initial stress and the temperature increase.

The effect of temperature on the strain rate acceleration factor for lead-free solders is shown in Fig. 8. The logarithmic strain rate acceleration factor ln Ω is plotted against the reciprocal temperature $1/T$. The magnitude of Ω decreases as the temperature increases. The following equation was deduced to express the magnitude of Ω:[10]

$$\Omega = A_s(\sigma_0/E)^{n_s}\exp(Q_s/RT), \quad (5)$$

where A_s, n_s, and Q_s are constants, provided that the normalized initial stress σ_0/E is used instead of σ_0. The relationship between ln Ω and $1/T$ appears to be linear, and the slope of the line gives the value Q_s/R. The constant Q_s of Sn-3.0Ag-0.5Cu is 7.2 kJ/mol under a constant stress of 7.8 MPa; the constant Q_s of Sn-7.5Zn-3.0Bi is 11 kJ/mol under a constant stress of 6.5 MPa. A_s, n_s, and Q_s are physically meaningless, but they are useful to try to complete the creep life assessment.

The value $\Omega/\exp(Q_s/RT)$ is plotted against the initial stress σ_0 in Fig. 9. All data points seem to fall in the vicinity of a single line. The slope of the line shows n_s. The parameter Ω is temperature dependent but less dependent on the initial stress. Table II shows the present experimental data of these constants, n_0, Q_0, n_s, and Q_s.

Creep Life Assessment

Rewriting Eq. 1 results in Eq. 6 as follows:

$$\dot{\varepsilon} = \dot{\varepsilon}_0 \exp(\Omega\varepsilon). \quad (6)$$

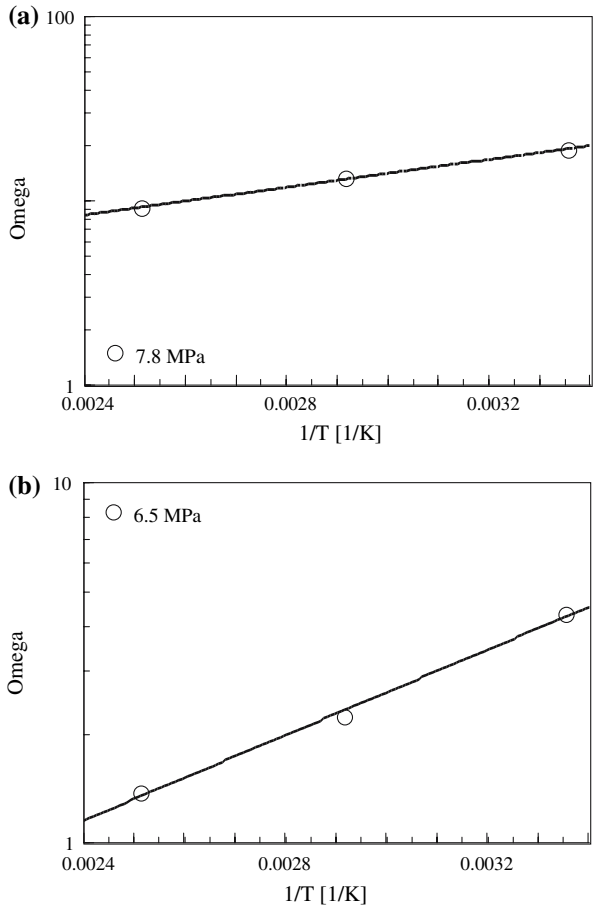

Fig. 8. Relationship between the strain rate acceleration factor and the reciprocal temperature for (a) Sn-3.0Ag-0.5Cu and (b) Sn-7.5Zn-3.0Bi.

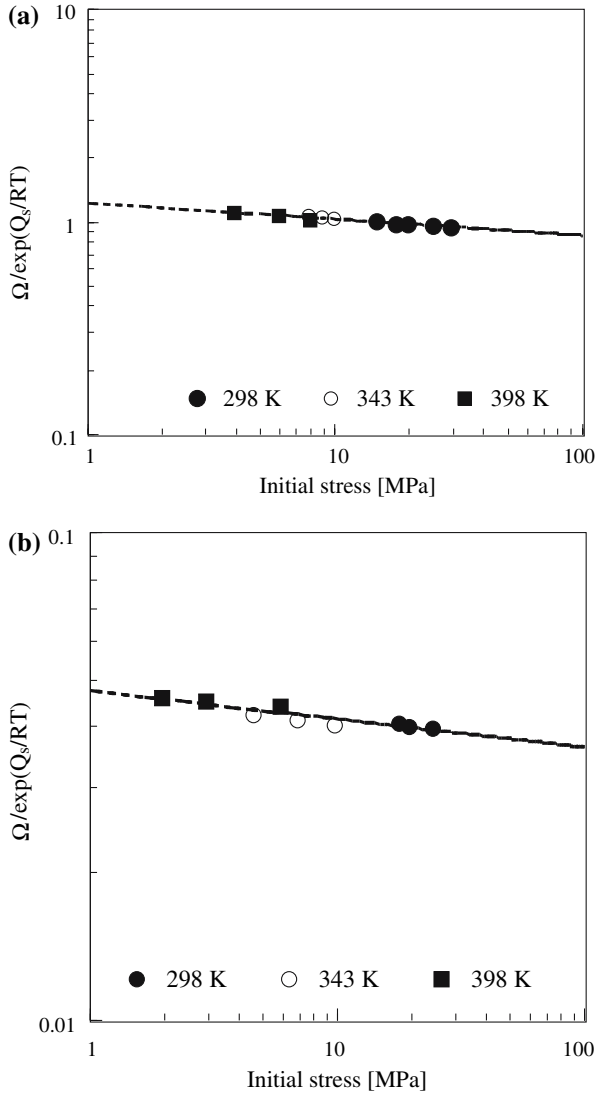

Fig. 9. Temperature-compensated strain rate acceleration factor as a function of the initial stress for (a) Sn-3.0Ag-0.5Cu and (b) Sn-7.5Zn-3.0Bi.

Integrating Eq. 6 with respect to time, from t to t_r, results in Eq. 7

$$t_r - t = (1/\Omega\dot{\varepsilon_0})[\exp(-\Omega\varepsilon) - \exp(-\Omega\varepsilon_r)], \quad (7)$$

where ε_r is the rupture strain. The magnitude of $\exp(-\Omega\varepsilon_r)$ is generally much smaller than $\exp(-\Omega\varepsilon)$, so Eq. 7 can be reduced to Eq. 8

$$t_r - t = (1/\Omega\dot{\varepsilon}). \quad (8)$$

Equation 8 suggests a very important result, that the product of the strain rate and the remaining life ($t_r - t$) is constant (1/Ω). So the remaining life of the lead-free solder can be calculated, if Ω and the strain rate are given.

Substituting t = 0 in Eq. 8 results in Eq. 3. Equation 3 is able to predict the creep rupture time of specimens if $\dot{\varepsilon_0}$ and Ω are known. The magnitude of $\dot{\varepsilon_0}$ and Ω can be estimated from Eqs. 4 and 5 as a function of temperature and stress. Therefore, the creep rupture time of specimens is predicted using Eq. 9

$$t_r = (A_s A_0)^{-1}(\sigma_0/E)^{-(n_0+n_s)}\exp[(Q_0 - Q_s)/RT], \quad (9)$$

if the temperature and initial stress are known. Figure 10 shows the relationship between the initial stress and the creep rupture time at each temperature. The data points are experimental results and the lines are described by Eq. 9. The creep rupture time decreases with the increasing initial stress and temperature. Equation 9 gives a good fit to the initial stress versus the creep rupture time at each temperature. The comparison of the calculated creep rupture time with the experimental results is shown in Fig. 11. The validity of Eq. 9 is shown in Fig. 11.

CONCLUSIONS

The creep properties of tin-based lead-free solders (Sn-3.0Ag-0.5Cu and Sn-7.5Zn-3.0Bi) were investigated at temperatures between 298 K and 398 K.

Table II. Values of the Constants Estimated in this Study for the Lead-Free Solders

	Q_0 (kJ/mol)	Q_s (kJ/mol)	n_0	n_s
Sn-3.0Ag-0.5Cu	108	7.2	7.8	-7.7×10^{-2}
Sn-7.5Zn-3.0Bi	83	11	3.1	-5.8×10^{-2}

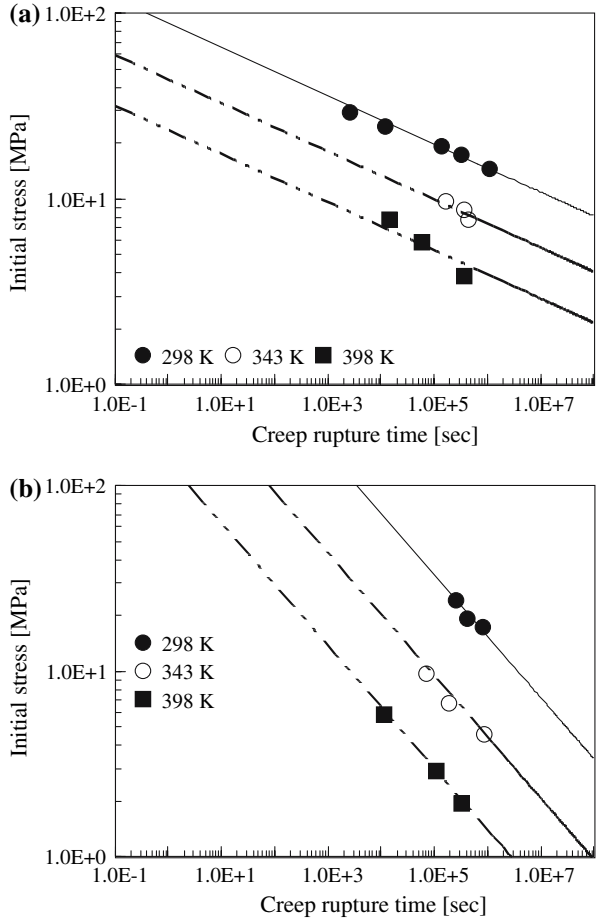

Fig. 10. Relationship between the initial stress and the creep rupture time for (a) Sn-3.0Ag-0.5Cu and (b) Sn-7.5Zn-3.0Bi.

The creep rupture time decreases as the initial stress and temperature increase. Applying the omega method to the analysis of creep curves of the tin-based, lead-free solders, the calculated creep curve accurately describes the creep deformation and the rupture point. The parameter $\dot{\varepsilon}_0$, which is the imaginary initial strain rate, increases as the initial stress and temperature increase. The apparent activation energy for $\dot{\varepsilon}_0$ is 108 kJ/mol in Sn3.0Ag0.5Cu and 83 kJ/mol in Sn-7.5Zn-3.0Bi. The remaining life of the lead-free solder can be calculated, if Ω and the strain rate are known. If the temperature and initial stress are known, the creep rupture time of specimens is predicted using $t_r = (A_s A_0)^{-1}(\sigma_0/E)^{-(n_0+n_s)}\exp[(Q_0 - Q_s)/RT]$.

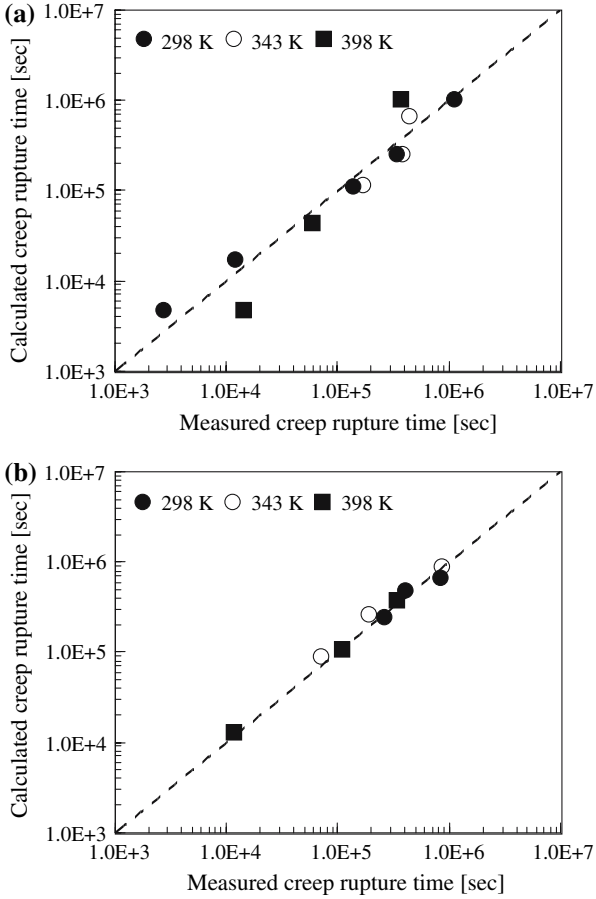

Fig. 11. Comparison of calculated creep rupture time with experimental results for (a) Sn-3.0Ag-0.5Cu and (b) Sn-7.5Zn-3.0Bi.

ACKNOWLEDGEMENTS

The help of Mr. T. Matsuda from Sumitomo Metal Technology Inc. in acquiring solder mechanical properties and many helpful discussions with Mr. E. Mukai, Research Center, DENKA, are gratefully acknowledged.

REFERENCES

1. C.M.L. Wu and M.L. Huang, *J. Electron. Mater.* 31(5), 442 (2002).
2. M.L. Huang, L. Wang, and C.M.L. Wu, *J. Mater. Res.* 17(11), 2897 (2002).
3. I. Shohji, C. Gagg, and W.J. Plumbridge, *J. Electron. Mater.* 33(8), 923 (2004).
4. M.L. El-Bahay, M.E. El Mossalamy, M. Mahdy, and A.A. Bahgat, *J. Mater. Sci.: Mater. Electron.* 15, 519 (2004).
5. Y. Kariya, M. Otsuka, and W.J. Plumbridge, *J. Electron. Mater.* 32(12), 1398 (2003).
6. J. Shi and T. Endo, *Tetsu-to-Hagane* 80(10), 795 (1994) (in Japanese).
7. J. Shi and T. Endo, *Scripta Metallurgica et Materialia* 32(8), 1159 (1995).
8. M. Prager, *J. Press. Vess. Technol.* 117, 95 (1995).
9. C. Coston and N.H. Nachtrieb, *J. Phys. Chem.* 68, 2219 (1964).
10. J. Shi, K. Tai, and T. Endo, *Tetsu-to-Hagane* 81(8), 839 (1995) (in Japanese).